Journal of Hazardous Materials 166 (2009) 1232–1237

Contents lists available at ScienceDirect

Journal of Hazardous Materials

journal homepage: www.elsevier.com/locate/jhazmat

Using tracer technique to study the flow behavior of surfactant foam

Yih-Jin Tsai*, Feng-Chih Chou, Shin-Jen Cheng

Department of Environment and Resources Engineering, Diwan University, No. 87-1, Nansh Li, Madou, Tainan, Taiwan

ARTICLE INFO

Article history:
Received 3 May 2008
Received in revised form 19 October 2008
Accepted 5 December 2008
Available online 11 December 2008

Keywords:
Tracer technique
Surfactant foam
Sandbox test
Iron powder
Foam flow

ABSTRACT

Surfactant foam was used to remove absorbed hydrocarbons from soils. The nature and extent of the foam pathway decide the efficiency of this technology. The characteristics and behavior of foam flow are difficult to visually observe. In this study, laboratory sandbox experiments were performed to estimate the flow behavior of surfactant foam and thus elucidate the properties and flow behavior of surfactant foam. To quantitatively determine the distribution of foam and evaluate accurately the flow field of foam in the soil, this study designed a special technique, applying micro-scale iron powder as a tracer. The foam generated with 4% (w/v) mixed solution of Span 60 and sodium dodecyl sulfate (SDS) showed an excellent stability and quality, which made it particularly apt for this study. The results indicated that the foam flows through the zone above the clay planes and also flows through the zone between the clay planes. The heterogeneous sand does not inhibit the invasion of foam flow. Moreover, the results of tracer tests and photographs of the foam distributions in sandbox were identical in the behavior of foam flow. This knowledge is valuable for providing insight into the foam remediation of contaminated soil.

1. Introduction

In recent years, there has been an increasing interest in the remediation of nonaqueous phase liquid (NAPL) source zones. NAPLs usually enter the unsaturated zone as discrete liquid phases, and move because of gravitational and capillary forces. Because of the low solubility of hydrophobic organic compounds in water, the residual organic phase usually represents a long-term contamination source for soil and groundwater. Owing to the tendency of contaminants to tightly bind or absorb onto the soil particles, subsurface contamination is complex and difficult to treat.

An effective remediation technique for subsurface contamination is the surfactant-solution flushing approach. This technique is primarily based on two processes. First, surfactants reduce the interfacial tension between water and contaminants that slows the mobility of the organic components. Therefore, surfactants are able to transfer the NAPLs to the mobile phase. Second, surfactant molecules in an aqueous solution can form micelles and increase the solubility of NAPLs in water. Numerous studies have indicated that aqueous surfactant solutions have been successfully used to remove absorbed hydrocarbons from soils [1–9].

Although surfactants have been effective in removing contaminants, large quantities of these chemicals are required. One way to reduce usage is to generate foam along with the surfactant solutions. Foam displays properties that are vastly different from the liquids that constitute the foam. This is because the foam has high volumes of air per unit volume. The density of foam is relatively low so that foam can easily overcome gravitational effects and be expected to flow much more freely than the liquid surfactant.

What are the foam–bubble microstructure and its pore-level schematic of foam flow? Kovscek et al. [10] indicated clearly that wetting liquid occupies the smallest pore spaces and clings to the surface of sand grains as wetting films due to strong capillary forces. The wetting phase maintains continuity throughout the pore structure. Minimal volumes of liquid transport as lamellae. Unshaded flowing foam transports as trains of bubbles through the largest and least-resistive flow channels. Because the smallest pore channels are occupied solely by wetting liquid and the largest pore channels carry flowing foam, significant bubble trapping occurs in the intermediate-sized pores. Bubbles and lamellae transport some distance are destroyed and then regenerated. No single bubble is conserved over any large distance.

Some scientists have focused on the contaminants removal by using surfactant foam. Rothmel et al. [11] performed a bench-scale study of surfactant foam, revealing that injecting the foam in a pulsed operation removed 75% of the contaminant. Jeong et al. [12] designed a special micromodel to study the remediation efficiency of surfactant foam. They reported that 99% of the residual trichloroethylene (TCE) was removed. Huang and Chang [13] used surfactant foam to remove n-pentadecane from a contaminated glass-bead column and evaluated its efficiency by comparing it with the results obtained by a surfactant-solution flooding process. It was found that the recovery of n-pentadecane increased significantly by using foam flooding than with surfactant-solution

* Corresponding author. Tel.: +886 6 5718888x318; fax: +886 6 5722858.
E-mail address: yjtsai@dwu.edu.tw (Y.-J. Tsai).

0304-3894/$ – see front matter © 2008 Elsevier B.V. All rights reserved.
doi:10.1016/j.jhazmat.2008.12.038

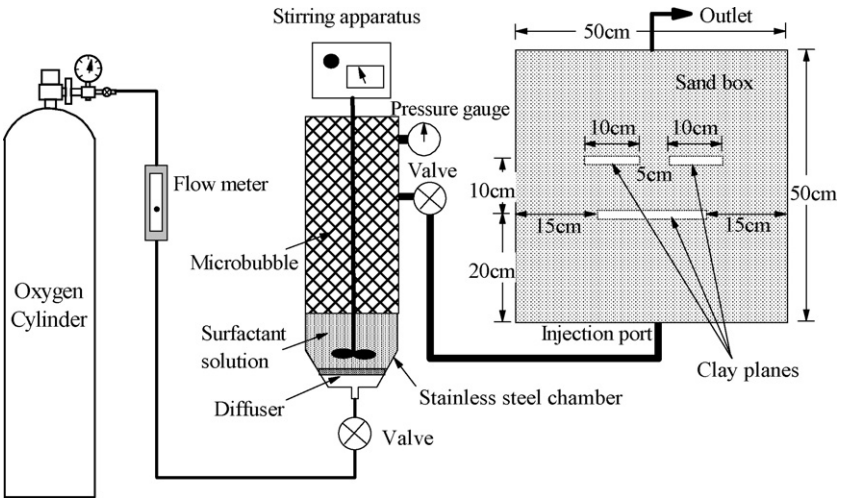

Fig. 1. Schematic experimental system of surfactant foam. This system is composed of an oxygen cylinder, a flow meter, a stainless steel chamber, a stirring apparatus, a pressure gauge, two valves, and a sandbox. Clay planes are settled only for heterogeneous sand test.

flushing. Mulligan and Eftekhari [14] investigated the capability of surfactants in the form of foam for removing the contaminant pentachlorophenol (PCP). They reported that Triton X-100 (1%) removed 85% and 84% of PCP from fine sandy soil and sandy-silt contaminated with 1000 mg/kg PCP, respectively. Wang and Mulligan [15] gave a comprehensive overview and evaluation of an emerging promising alternative, surfactant foam technology. They indicated that the surfactant foam is an innovative technology. There are many factors to be investigated for future development. Soil matrix characteristics, contaminant speciation, effectiveness of pulsed operation, and surfactant partitioning must be thoroughly analyzed to determine the applicability and effectiveness of in situ foam flushing to the subsurface conditions [15].

For the study of the behavior of surfactant foam, Chowdiah et al. [16] performed a column test and indicated that the foam behaved as highly viscous fluids when flowing through soils. However, the detailed behavior of surfactant foam and the affection of the soil matrix characteristics during foam injection have seldom been studied. Understanding the influence of soil matrix characteristics in foam flow is very important for subsurface remediation.

The objective of this research was to determine if the utilization of powder as a tracer allowed the visualization of foam flow in a laboratory sandbox. To achieve this purpose, laboratory sandbox experiments were performed to estimate the flow behavior of surfactant foam in soil. To overcome the high complexity and uncertainty of soil and for simplifying this test, quartz sand and clay were used for flow field evaluation. This study designed a novel and special experimental method to evaluate the flow field of foam in the sandbox. The results of these tests show that the flow of foam was able to be visualized using iron powder as a tracer in two laboratory sandbox experiments.

2. Experimental methods

2.1. Microbubble generator design and setup

In this study, as shown in Fig. 1, the generator is composed of a stainless steel chamber of 10 cm in diameter and 40 cm in height, a stirring apparatus (model DC-2R, Sun-Great Technology Co.), an oxygen cylinder, a flow meter (model RMA, Dwyer Instruments Inc.), and two valves. This design allows the use of oxygen and can generate suspensions with higher gas contents. The chamber is tightly closed with the stirring apparatus inside and pressurized using compressed gas. In this study, the surfactant solution of appropriate amount was injected into the chamber first. The stirring apparatus stirs the solution at a rate of about 300 rpm for 10 min. Then oxygen was injected at a rate of 300 ml/min, was passed through a diffuser. The diffuser had a pore size of 5 μm and was installed on the bottom of the stainless steel chamber. The stirring apparatus splits the injected gas into microbubbles that are stabilized by the surfactant.

2.2. Surfactants selection and foam tests

Surfactants are a class of natural and synthetic chemicals that promote the wetting, solubilization, and emulsification of various types of organic and inorganic contaminants. They are amphiphilic molecules with both hydrophilic and hydrophobic portions. Therefore, many surfactants, depending on concentration and surfactant type, act as a bridge between the air and liquid interface, thereby reducing the surface tension of water. Wan et al. [17] reported that the generation of long-lasting and stable microbubble suspensions is accomplished using a mixture of sodium dodecyl sulfate (SDS) and sorbitan monostearate (Span 60). After evaluating 10 different commercial surfactants for their ability to foam, Mulligan and Eftekhari [14] reported that octylphenol ethoxylate ether (Triton X-100) generated foam with higher stability and quality.

In this study, sandbox tests were conducted with a stable and highly concentrated microbubble suspension. This study refers to the foregoing study on Triton X-100 and a mixture of SDS and Span 60. These were evaluated for their stability and quality to foam. The active contents for Triton X-100 and SDS used herein are reported to be 99 wt.% by Merck Schuchardt OHG, Germany. Span 60 is 100 wt.% as reported by Kanto Chemical Co., Japan.

The physical structure of the foam and many of the properties depend on the relative proportion of gas and liquid constituting the foam. The foam quality is a term used to specify the gas content of the foam. It is defined as

$$\text{Foam Quality} = \frac{\text{Gas Volume}}{\text{Total Foam Volume}} \quad (1)$$

The overall question of foam stability requires the consideration of both the static and dynamic aspects of bubble interactions. Foam stability reflects the ability of the foam to resist bubble collapse. It can be quantified by the time required for collapsing half of the foam [16].

Table 1
Statistical results of foam quality and stability for Triton X-100 and Span 60/SDS without and with iron powder.

Concentration	Without iron powder				With iron powder			
	Span 60/SDS		Triton X-100		Span 60/SDS		Triton X-100	
	Quality (%)	Stability (min)	Quality (%)	Stability (min)	Quality (%)	Stability (min)	Quality (%)	Stability (min)
0.20%	94.1 ± 0.2	36.6 ± 2.1	96.2 ± 0.5	66.0 ± 1.8	96.2 ± 0.3	25.0 ± 1.3	98.2 ± 0.5	6.2 ± 0.6
0.80%	95.2 ± 0.3	40.4 ± 2.9	93.8 ± 0.3	77.3 ± 2.8	96.8 ± 0.3	53.3 ± 2.6	98.7 ± 0.4	8.6 ± 0.9
1.40%	96.4 ± 0.5	45.0 ± 2.2	96.0 ± 0.3	36.4 ± 2.0	93.2 ± 0.4	88.3 ± 2.4	96.8 ± 0.5	7.8 ± 0.5
2.00%	93.8 ± 0.4	48.8 ± 3.7	96.1 ± 0.2	36.4 ± 2.4	94.1 ± 0.2	90.0 ± 3.7	96.1 ± 0.3	7.9 ± 0.7
3.00%	95.3 ± 0.6	75.0 ± 3.2	97.1 ± 0.4	34.8 ± 1.5	92.8 ± 0.4	98.0 ± 3.3	–	–
4.00%	96.4 ± 0.6	134.0 ± 3.9	94.4 ± 0.3	35.9 ± 2.1	88.5 ± 0.3	129.2 ± 4.3	–	–

2.3. Application of iron powder

Observing the flow field of foam in the porous media is challenging because of the invisibility of porous media. The method used to estimate the flow field or distribution of injected foam is very important for soil remediation. This study used the commercial iron powder with grain size around 10 μm (above 99.5%, Merck KGaA, Germany) and was mixed with the surfactant solution to obtain an iron suspension of 3.4% by weight. Then this suspension was used to generate the foam by microbubble generator. Besides, sodium oleate (above 95%, Hayashi Pure Chemical Industries Ltd., Japan) of 0.4% was used to enhance the bond between the iron particles and bubbles. Iron particles moved together with the bubbles and propagated through the soil. Accordingly, the iron particles can be considered as the tracer material of the foam flow.

2.4. Sandbox setup and test

To study flow behavior of surfactant foam, experiments were performed in a two-dimensional Plexiglas sandbox. The sandbox was constructed from 1 cm thick Plexiglas and was 5 cm wide by 50 cm long by 50 cm high (internal dimensions). The front and back walls were fastened together with bolts. The bolts were spaced 10 cm apart and placed at the tank boundaries. Additionally, the front and back walls were reinforced against flexure with bolts. An injection port and an outlet port were placed, respectively, near the bottom and top at the center of the sandbox.

The quartz sand used herein was 99 wt.% in purity and manufactured by Chin Ching Co., Ltd.; grain size ranged from 0.60 mm to 0.85 mm. The sand had to be mixed adequately before packing. The sandbox was lying on the table without front wall. The mixed sand was added to the sandbox quickly. Then the added sand was compressed into a compacted-sand and the front wall was fastened on the sandbox. The dry packing procedure herein was important in simulating the homogeneous compacted-sand. For the heterogeneous sand, three clay planes were used in this study (as seen in Fig. 1). One plane was 2 cm thick by 20 cm wide and was installed at a height of 20 cm from the bottom. The other two planes were 2 cm thick by 10 cm wide and were installed at a height of 30 cm from the bottom of sandbox. The space between these two planes was 5 cm.

The foam with iron particles was injected at a rate of about 300 ml/min into the sandbox from the injected port. The foam injection process was conducted for about 10 min and the foam visually filled the sandbox. The sandbox was opened and the compacted sand was segmented into 100 samples of equivalence. The sand samples were dried in a sand oven at 105 °C for 8 h. Then, the iron particles were separated by magnet from each sand sample and the weights of the iron particles and sand were measured. By using these weight data, the iron contained in each sand sample in percentage was obtained.

3. Results and discussion

3.1. Analysis of foam quality and stability

3.1.1. Triton X-100

Foam of Triton X-100 of different concentrations (0.2–4%) with and without iron particles was generated. Table 1 shows that the qualities range between 93.8 ± 0.3% and 97.1 ± 0.4% for the foam without iron particles, and range between 96.1 ± 0.5% and 98.2 ± 0.3% for the foam with iron particles (3.4% by weight). These results indicated that the addition of iron particles and surfactant concentration did not vary foam quality evidently for Triton X-100. The stability of foam is defined as the time required for the drainage of half of the liquid volume. Table 1 also shows that stability does not relate to the concentration of Triton X-100. Furthermore, compared to the stability of foam without iron particles, the stability of foam with iron particles decreases evidently. For both with and without iron particles, Triton X-100 of concentration 0.8% has a highest foam stability of 8.6 ± 0.9 min and 77.3 ± 2.8 min, respectively. This result of foam stability indicated that the combination of sodium oleate and iron particles significantly decrease the strength of foam film.

3.1.2. Span 60 and SDS

The quality and stability of foam for the mixed solutions of Span 60 and SDS are demonstrated in Table 1. The qualities range from 93.8 ± 0.4% to 96.4 ± 0.6% and the stability varied from about 36.6 ± 2.1 min and 134.0 ± 3.9 min. Table 1 also shows that the quality of foam with iron particles (3.4% by weight) was similar to that without iron particles. However, the addition of sodium oleate and iron particles slightly increased the stability of foam. A mixed solution of Span 60 and SDS with a concentration of 4.0% has a higher foam stability of 129.2 ± 4.3 min and 134.0 ± 3.9 min for both with and without iron particles, respectively. Besides, the results also indicated that the stability relates to the concentration of Span 60 and SDS. In the case of Span 60 and SDS mixed solutions, the declining foam stability correlates with declining concentration of surfactants. Unlike the Triton X-100 solutions, declining foam stability does not appear to be dependent upon inherent properties.

According to the results of the foam quality and stability test, Span 60 and SDS mixed solution of a concentration of 4% can generate the most stable foam, especially for the foam with iron particles. Span 60 is a solid hydrophobic surfactant and SDS is a water-soluble surfactant. Such a combination stabilizes bubbles by the formation of a solid-condensed monolayer at the gas–water interface. The tight packed monolayer can sustain the attachment of the solid iron particles to the bubbles and slow diffusive gas loss. Hence, this combination yielded the more stable foam than Triton X-100. This study used a 4% Span 60 and SDS solution mixed with iron particles of 3.4% and sodium oleate of 0.4% by weight to generate the foam and the sandbox tests were performed.

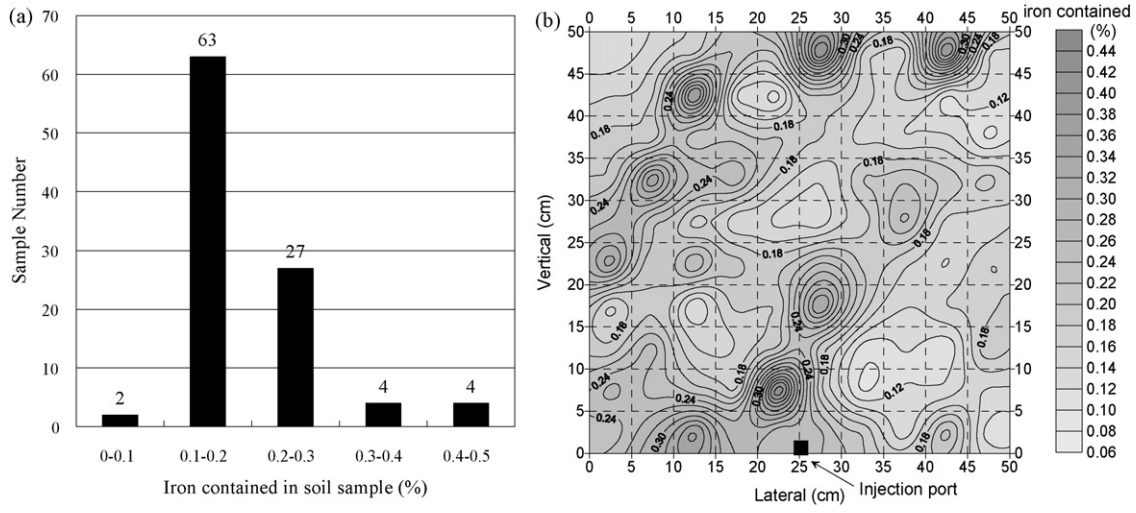

Fig. 2. Experimental results of foam injected test in homogeneous sand: (a) bar chart of sample number for iron particles contained in sand samples; (b) contour map of the iron particles contained in sand samples.

3.2. Sandbox test

3.2.1. The flow behavior of surfactant foam in homogeneous sand

The result of percentage of iron particles in homogeneous sand is shown in Fig. 2(a). The result indicates that among 100 samples, 63 sand samples contain iron particles ranging from 0.1% to 0.2%. Twenty-seven sand samples contain iron particles ranging from 0.2% to 0.3%. The maximum value of iron particles contained in the sand sample is 0.45%. That is, 90% of the sand samples contain iron particles ranging from 0.1% to 0.3%.

The grid estimation of iron in sand samples for homogeneous sand was completed by the Kriging method and anisotropic semivariogram analysis. These estimated results showed that the main flow direction was 60° (rightward and upward) and the secondary flow direction was between 150° and 180° (leftward and upward). Fig. 2(b) shows the contour of iron particles contained in quartz sand after foam was injected. This figure presents variations of contained iron particles. The maximum iron contained was around 0.4% at (22.5, 7.5), (12.5, 42.5), (27.5, 47.5), and (42.5, 47.5). The minimum was around 0.1% at (32.5, 7.5) and (47.5, 37.5). A higher ratio of iron indicates where the foam density is higher. On the basis of this contention, the injected foam flowed radially from the inlet port. Fig. 2(b) indicates that the injected foam flowed leftward slightly more than rightward. One preferential flow flowed leftward and upward to the left boundary during the initial stage. At the same time, one preferential flow flowed rightward and upward from the injection port. Besides, another preferential flow occurred and flowed rightward and upward to the up boundary when the foam contacted with the left boundary. However, the result seen in Fig. 2(b) indicates that the foam also passed through all the sample blocks under the occurrence of preferential flow. Almost all the sand samples contained iron particles exceeding 0.1%.

Although this test was to explore the flow behavior of surfactant foam in homogeneous sand, the preferential flow was occurred during this test. This result was due to the blockage phenomena in porous medium [18] and caused the heterogeneous effect in this test. Tang and Kovscek [19] reported that a significant fraction of the gas-phase was stationary during steady-state foam flow in sandstone. Nguyen et al. [20] indicated that foam mobility distribution was non-uniform in granular porous media. Foam mobility increased from the center to the boundary and some of surfactant foam was trapped in porous within the flow domain. Accordingly,

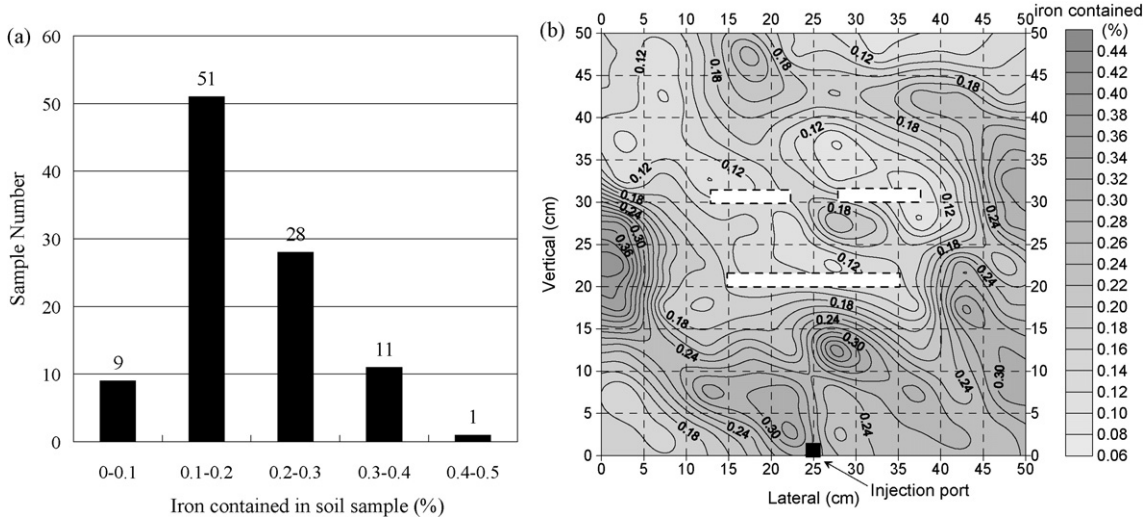

Fig. 3. Experimental results of foam injected test in heterogeneous sand: (a) bar chart of sample number for iron particles contained in sand samples; (b) contour map of iron particles contained in sand samples.

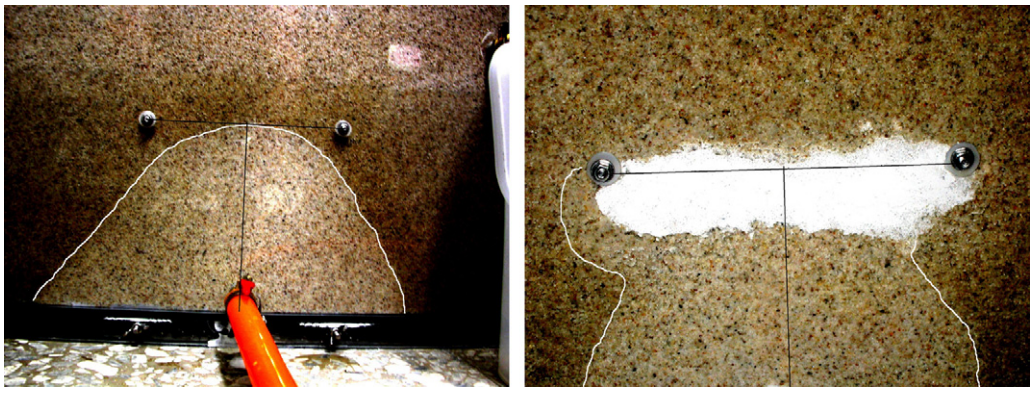

Fig. 4. Photographs of the foam distribution in sandbox at 3 min after startup for (a) homogeneous sand and (b) heterogeneous sand. The white line in both (a) and (b) indicates the front of foam and the white block of (b) indicates the clay plane.

the blockage effect in porous medium is evidently occurred during the foam flow. This phenomenon also confirms the non-uniform flow behavior of foam in this test.

3.2.2. The flow behavior of surfactant foam in heterogeneous sand

The result of percentage of iron particles in heterogeneous sand is shown in Fig. 3(a). The result indicates that among 100 samples, 51 sand samples contain iron particles ranging from 0.1% to 0.2%. Twenty-eight sand samples contain iron particles ranging from 0.2% to 0.3%. Almost 80% of the sand samples contain iron particles ranging from 0.1% to 0.3%. The maximum value of iron particles contained in the sand sample is 0.41%.

According to results of the Kriging method and anisotropic semivariogram analysis, these estimated results showed that the main flow direction is 150° (leftward and upward) and the secondary flow direction is 60° (rightward and upward) for the heterogeneous sand. Fig. 3(b) shows the distribution of percentage of iron particles in quartz sand after foam was injected in this experiment. This figure also shows the location of three clay planes. The maximum iron contained was 0.41% at (2.5, 22.5). The minimum was around 0.1% at (2.5, 7.5), (2.5, 37.5), (7.5, 42.5), (27.5, 35), and (37.5, 27.5). Fig. 3(b) also shows that the three clay planes were installed at 20 and 30 cm in height from the bottom of sandbox. The clay planes changed the flow behavior of foam significantly. The injected foam flowed radially from the injection port and extended its semicircle gradually. Similar to the initial flow style in homogeneous sand, the injected foam flowed leftward slightly more than rightward. When the front of foam contacted with the clay plane at a height of 20 cm, the clay plane divided the foam into left and right parts. The left foam flowed leftward and upward to the top boundary. The clay pushed the right foam flow rightward; later the foam flowed leftward and upward again to the outlet of top boundary. Besides, the right foam was divided clearly when the foam contacted with the right clay plane at height of 30 cm. The clay planes changed the flow behavior of surfactant foam. However, the foam flowed into the zone between clay planes. Most of the sand samples between and around the clay planes contained iron particles exceeding 0.1%. The heterogeneity of sand influences the behavior of foam flow. However, the characteristic of foam flow, that is, the radial flow, permits the foam to flow horizontally and downward into the zone above the clay planes.

Kovscek et al. [18] considered noncommunicating and communicating layers where the gas fractional flow was high, greater than 97%, and the permeability contrast was 10:1. Good diversion to the low-permeability layer was predicted and gas breakthrough occurred first in the low-permeability system. They also reported that the degree of diversion to the low-permeability layer depends on the details of foam trapping as a function of permeability. Besides, Kovscek and Bertin [21] designed an experimental system for performing heterogeneous foam-displacement experiments. Their results also confirmed that foamed gas can be more mobile in lower permeability porous media. Accordingly, this phenomenon supports the results of foam flow observed in the heterogeneity sand.

In comparing Figs. 2 and 3, 94% and 90% of samples contain the iron particles ranging from 0.1% to 0.4% for homogeneous and heterogeneous sand, respectively. For the zone above the clay planes, most of the zone contains the iron particles ranging from 0.1% to 0.2% for homogeneous sand. For heterogeneous sand, most of zone also contains the iron particles ranging from 0.1% to 0.2%. This result indicates that the zone above the clay planes does not vary seriously. The blockage phenomenon in porous medium causes the heterogeneous effect for both homogeneous and heterogeneous sand. The foam flows through the zone above the clay planes and also flows through the zone between the clay planes. Under the effect of blockage in porous medium, the difference of foam behavior between homogeneous and heterogeneous sand is not significant. Besides, foam is less mobile towards the outlet for both homogeneous and heterogeneous sandbox test.

3.3. Analysis of mass balance

For homogeneous sand, the iron powder in suspension was 30.00 g. The residual iron powder, which was not injected into sandbox, was 10.74 g. The total iron powder collected from 100 sand samples was 19.47 g after the test. Accordingly, the weights of iron powder were 30.00 g and 30.21 g before and after the test, respectively. The recovery and error were 100.7% and 0.7% in this test. The probably reason for the tiny increasing in weight after the test was that the oxide formed on the surface of iron particles during the test. For heterogeneous sand, the iron powder in suspension was 25.00 g. The residual iron powder was 7.97 g. The iron powder collected from 100 sand samples was 17.34 g after the test. Accordingly, the weights of iron powder were 25.00 g and 25.31 g before and after the test, respectively. The recovery and error were 101.2% and 1.2% in this test. The smallness of the errors implies that both tests yielded results that preserve mass balance.

3.4. Results validation

In this study, the observing the flow field of foam in sandbox was a difficult work too. The front of foam was visually differentiated only at the first few minutes after startup. Fig. 4 shows the photographs of the distributions of injected foam at 3 min after startup (the white line indicates the front of foam). Fig. 2(b) shows that the foam flows radially but there are three main preferential flows. Fig. 4(a) indicates that the left half zone of the injected foam is greater than that of right half zone. In other words, the foam flows leftward slightly more and easily than rightward. The results

seen in Fig. 4(a) and Fig. 2(b) are identical in the behavior of foam flow. Moreover, Fig. 4(b) shows that the left half zone of the foam is greater than that of right half zone for heterogeneous sand. This result is similar to the result seen in Fig. 3(b) too. The estimated results of Kriging method also show that the main flow direction is 150° (leftward and upward). In Figs. 2 and 3, the main effect of sand property in surfactant foam flow behavior is the change in the direction of flow. The results seen in Figs. 2–4 indicate the distribution of iron powder reflected the accurate result of foam flow behavior, including the flow direction and preferential flow.

4. Conclusion

Experimental sandbox tests of foam flow in homogeneous and heterogeneous porous media were performed. The results of this study indicated that the difference of foam behavior between homogeneous and heterogeneous sand was not significant under the effect of blockage in porous medium. Besides, foam was less mobile towards the outlet for both homogeneous and heterogeneous sandbox test.

Estimating the flow field or distribution of injected foam is very important for applying surfactant foam in remediating the contaminated soil. Some scientists used X-ray coupled with tracer gas to estimate the foam distribution [20,21]. It is a good but pricey method. This study used commercial iron powder as the tracer material of foam flow. The results seen in Figs. 2–4 indicated that the iron powder successfully flowed with surfactant foam. The distribution of iron powder reflected the accurate result of foam flow behavior, including the flow direction and preferential flow. These characteristics and behavior of foam flow are difficult to visually observe. This tracer technique offers some believable data about the characteristics and changes of the foam flow. Moreover, iron powder can be easily separated from other materials just using a small magnet instead of a pricey apparatus. The most important is that this method could be easily applied in a large-scale field test for studying the foam flow behavior and expands our understanding in foam flow.

Acknowledgements

The authors thank Dr. Hsing-Lung Lien for his comments in this study. The technical assistance of Tsu-Chi Chen and Chin-Yang Wu is also greatly appreciated.

Appendix A. Supplementary data

Supplementary data associated with this article can be found, in the online version, at doi:10.1016/j.jhazmat.2008.12.038.

References

[1] O.K. Gannon, P. Bibring, K. Raney, J.A. Ward, D.J. Wilson, J.L. Underwood, K.A. Debelak, Soil clean up by in-situ surfactant flushing. III. Laboratory results, Sep. Sci. Technol. 24 (1989) 1073–1094.
[2] B.W. Vigon, A.J. Rubin, Practical considerations in the surfactant-aided mobilization of contaminants in aquifers, J. Water Pollut. Control Federat. 61 (1989) 1233–1240.
[3] C.C. Ang, A.S. Abdul, Aqueous surfactant washing of residual oil contamination from sandy soil, Ground Water Monit. Remediat. 11 (1991) 121–127.
[4] A.S. Abdul, T.L. Gibson, Laboratory studies of surfactant-enhanced washing of polychlorinated biphenyl from sandy material, Environ. Sci. Technol. 25 (1991) 665–671.
[5] A.S. Abdul, T.L. Gibson, C.C. Ang, J.C. Smith, R.E. Sobczynski, In situ surfactant washing of polychlorinated biphenyls and oils from a contaminated site, Ground Water 30 (1992) 219–231.
[6] K.D. Pennell, L.M. Abriola, W.J. Weber Jr., Surfactant-enhanced solubilization of residual dodecane in soil columns. 1. Experimental investigation, Environ. Sci. Technol. 27 (1993) 2332–2340.
[7] A.S. Abdul, C.C. Ang, In situ surfactant washing of polychlorinated biphenyls and oils from a contaminated field site: phase II pilot study, Ground Water 32 (1994) 727–734.
[8] J.C. Fountain, R.C. Starr, T. Middleton, M. Beikirch, C. Taylor, D. Hodge, A controlled field test of surfactant-enhanced aquifer remediation, Ground Water 34 (1996) 910–916.
[9] V. Dwarakanath, K. Kostarelos, G.A. Pope, D. Shotts, W.H. Wade, Anionic surfactant remediation of soil columns contaminated by nonaqueous phase liquids, J. Contam. Hydrol. 38 (1999) 465–488.
[10] A.R. Kovscek, T.W. Patzek, C.J. Radke, A mechanistic population balance model for transient and steady-state foam flow in boise sandstone, Chem. Eng. Sci. 50 (1995) 3783–3799.
[11] R.K. Rothmel, R.W. Peters, St.E. Martin, M.F. Deflaun, Surfactant foam/biodegradation of in situ treatment of TCE-DNAPLs, Environ. Sci. Technol. 32 (1998) 1667–1675.
[12] S.W. Jeong, M.Y. Corapcioglu, S.E. Roosevelt, Micromodel study of surfactant foam remediation of residual trichloroethylene, Environ. Sci. Technol. 34 (2000) 3456–3461.
[13] C.W. Huang, C.H. Chang, A laboratory study on foam-enhanced surfactant solution flooding in removing n-pentadecane from contaminated columns, Colloids Surf. A 173 (2000) 171–179.
[14] C.N. Mulligan, F. Eftekhari, Remediation with surfactant foam of PCP-contaminated soil, Eng. Geol. 70 (2003) 269–279.
[15] S. Wang, C.N. Mulligan, Rhamnolipid foam enhanced remediation of cadmium and nickel contaminated soil, Water Air Soil Pollut. 157 (2004) 315–330.
[16] P. Chowdiah, B.R. Misra, J.J. Kilbane II, V.J. Srivastava, T.D. Hayes, Foam propagation through soils for enhanced, in-situ remediation, J. Hazard. Mater. 62 (1998) 265–280.
[17] J. Wan, S. Veerapaneni, F. Grdelle, T.K. Tokunaga, Generation of stable microbubbles and their transport through porous media, Water Resour. Res. 37 (2001) 1173–1182.
[18] A.R. Kovscek, T.W. Patzek, C.J. Radke, Mechanistic foam flow simulation in heterogeneous and multidimensional porous media, Soc. Petrol. Eng. J. 2 (1997) 511–526.
[19] G.Q. Tang, A.R. Kovscek, Trapped gas fraction during steady-state foam flow, Trans. Porous Med. 65 (2006) 287–307.
[20] Q.P. Nguyen, P.K. Currie, M. Buijse, P.L.J. Zitha, Mapping of foam mobility in porous media, J. Petrol. Sci. Eng. 58 (2007) 119–132.
[21] A.R. Kovscek, H.J. Bertin, Foam mobility in heterogeneous porous media. II. Experimental observations, Trans. Porous Med. 52 (2003) 37–49.